Polymer Journal, Vol. 37, No. 3, pp. 192–205 (2005)

Segmental Orientation under Simultaneous Biaxially Stretching using a Lattice Model and Application of Oriented Crystallization of Ultra-high Molecular Weight Polyethylene Films Prepared by Gelation/Crystallization from Solution

Yuezhen BIN,[1] Ai KOGANEMARU,[1] Teruo NAKASHIMA,[2] and Masaru MATSUO[1,†]

[1]*Department of Textile and Apparel Science, Faculty of Human Life and Environment, Nara Women's University, Kitauoya, Nishi-machi, Nara 630-8263, Japan*
[2]*Faculty of Agriculture, Kinki University, 3327-204 Nakamachi, Nara 631-8505, Japan*

(Received September 17, 2004; Accepted December 14, 2004; Published March 15, 2005)

ABSTRACT: A lattice model proposed before for uniaxial stretching of polyethylene films was applied to estimate the oriented crystallization of ultra-high molecular weight polyethylene (UHMWPE) dry gel films under simultaneous biaxially stretching. In this model system, the preferred axis associated with the preferred orientation of amorphous chain segments was chosen along the direction between two successive cross-linked points and the preferred axis was assumed to deform in an affine fashion with respect to the stretching direction. As the application of the proposed model, the orientation distribution function of crystallites was calculated on the basis of the lattice model and oriented crystallization model. The oriented crystallization model is based on the concept that a kinetically determined distribution of crystal chain axes as the normalized distribution of clusters found at the saddle point corresponding to a non-uniform orientation under conditions of a steady-state nucleation rate. Of course, the crystallites are oriented randomly with respect to the film normal direction. The parameter fitting for the formulated orientation distribution function of crystallites was done for the film which was prepared by the gelation/crystallization from solution with 0.9 g/100 mL concentration, the solvent being decalin, since the concentration assured the highest drawability under simultaneous biaxially stretching. The calculated orientation distribution functions $2\pi q_j(\cos\theta_j)$ of the reciprocal lattice vector of the crystal planes were in good agreement with the observed ones. Thus the numerical calculations indicate that the orientation of the *c*-axes depends on that of amorphous chain segments and the orientation behavior of crystallites is strongly affected by their rotation around the *c*-axis. [DOI 10.1295/polymj.37.192]

KEY WORDS A Lattice Model / Simultaneous Biaxially Stretching / Preferred Orientation / A Steady-State Nucleation Rate / Orientation Distribution Function of Crystallites /

Segmental orientation in uniaxially deformed elastomatic networks has been treated in terms of gas-like theories and liquid-like theories.[1–4] In the gas-like theories, the chain vector and segment vector distributions have been estimated theoretically by using idealized models in which the effect of mutual interference between chain segments are neglected. On the other hand, in a liquid-like theory,[3,4] the effect of intermolecular interferences relating to orientation-dependent packing entropy was taken into consideration based on a lattice model. Erman *et al.*[5,6] have attempted to improve the liquid-like theory by considering the effect of chain stiffness on segmental orientation. For this purpose, they adopted the lattice theory of Flory[7,8] for chains with freely jointed rod-like segments and applied it to a thermotropic system with anisotropic polarizabilities. Namely, Erman *et al.* pointed out that a segment of polyethylene chains with 1–22 bonds may be viewed as a rod-like object on the basis of the concept of Flory and Yoon[9] that a more rigorous analysis of the equivalent segment size of a freely jointed chain for polyethylene by matching the higher order moments of the end-to-end distance of the real and freely jointed chain leads to $m_r/m \approx 20$–22 (m_r = the number of segments in a real chain and m = the number of Kuhn segments). Their treatments[5,6] are of interest to understand the detailed phenomena of molecular orientation of actual polymeric materials under elongation. In their model system, the length-to-width ratio x of each segment of a chain, which is a measure of chain stiffness, is incorporated into the theory of segmental orientation. They introduced intermolecular contributions in networks with flexible chains as well as thermotropic effects between segments which result in phase transitions due to orientation upon stretching and formulated the second-order orientation factor associated with the second term of the Legendre function.

However, their treatment, which is essentially correct in terms of Helmholtz free energy, cannot be applied to polymer films, since the calculated second order orientation factor took a positive value in an un-

†To whom correspondence should be addressed (Tel&Fax: +81-742-20-3462, E-mail: m-matsuo@cc.nara-wu.ac.jp).

deformed state ($\lambda = 1$) at larger values of x. Of course, except for films, it is well-known that beyond a critical axial ratio x_c, systems of rod-like particles spontaneously split into two phases with different anisotropy, since the existing entropic driving forces are supplemented by an orientation-dependent energetic contribution. To explain this phenomenon, Flory *et al.*[7,8] have taken the preferred axis of a given domain along one of the principle axes of the lattice for liquid crystal systems and of hard rods dispersed in a dilute solution. Based on the same concept, Erman *et al.*[5] chose the preferred direction, which allows the preferential orientation of a segment, to the stretching direction. This leads to an abnormal phenomenon where polymer chains within a film are oriented without elongation in order to minimize the free energy.

In previous paper,[10] a modified model was proposed to solve this contradiction for polymer films, in which the preferred axis was chosen along the direction between two successive cross-link points. The modified model was mainly employed to analyze the orientation distribution function of amorphous chain segments of polyethylene during the process of oriented crystallization. The orientation of the preferred axis was assumed to behave as an affine fashion under elongation and the treatment was formulated in terms of the orientation distribution function with respect to the stretching direction by the application of the Legendre addition theorem.

The same treatment is applied to the orientation of crystallites on simultaneous biaxially stretching films, since analysis of the oriented crystallization of the film is very important for the production of crystalline polymer films. In doing so, this paper adopts the orientation distribution functions of the reciprocal lattice vectors of crystal planes measured elsewhere.[11,12] The simultaneous biaxially stretching was carried out using ultra-high molecular weight polyethylene (UHMWPE) dry gel films prepared by gelation/crystallization from solutions.[11–15]

EXPERIMENTAL

Experimental Method

The sample used in this experiment were UHMWPE (Hercules 1900/90189) with a viscosity-average molecular weight ($\bar{M}_v$) of 6×10^6. The solvent was decalin. The concentration of UHMWPE was 0.9 g/100 mL assuring the highest draw ratio.[11] Decalin solutions were prepared by heating the well-blended polymer-solvent mixture at 135 °C for 40 min under nitrogen, The solution was stabilized with 3% w/w of antioxidant (di-*t*-butyl-*p*-cresol) against UHMWPE. The hot homogenized solution was quenched to room temperature by pouring it into an aluminum tray, thus generating a gel. The decalin was allowed to evaporate from the gels under ambient conditions. The resulting dry gel film was vacuum-dried for 1 d to remove residual trace of decalin. The dry gel film was cut into a strip of 90×90 cm, The specimen was held at 150 °C for 5 min and elongated biaxially to the desired draw ratio using Iwamoto biaxial stretcher.

The X-ray diffraction measurements were carried out with a 12 kW rotating anode X-ray generator (Rigaku RDA-rA) operated at 200 mA and 40 kV. The film thickness of the films beyond 6×6 is less than 5 μm and it is very difficult even to obtain the orientation distribution function concerning the (110) and (200) planes with very strong diffraction intensity. Accordingly, we adopted a small but refined instrument to stack a number of thin films as shown in Figure 1.[11] In such a stacked condition, measurements of the X-ray diffraction intensity could be performed by using a horizontal scanning type goniometer, operating at a fixed time step scan of 0.1/40 s over a range of twice the Bragg angle $2\theta_B$ from 15 to 60° and from 70 to 79°. The intensity distribution was measured as a function of a given rotational angle θ_j by rotating about the stretching direction at 2–5° intervals fro 0 to 90° in Figure 1a and b, respectively.[11]

Characteristics of Test Specimens

To facilitate understanding the theoretical analysis, the characteristics of the original samples are shown in Table I and Figure 2, although they were shown elsewhere.[10] Table I summarizes change in melting point and crystallinity as a function of draw ratio. Upon the initial draw ratio from 1×1 (un-drawn) to 2×2, crystallinity and melting point decreases indicating the crystal transformation process from a folded to a fibrous type. Furthermore, in spite of an increase in crystallinity with increasing draw ratio, the corresponding melting point decreases indicating that the crystallites become less unstable.

Figure 2 shows small angle X-ray scattering (SAXS) and wide angle X-ray diffraction (WAXD) patterns for the original (un-deformed) dry gel film, when an incident beam was directed parallel to the film surface (end view). The WAXD pattern reveals the preferential orientation of the *c*-axes perpendicular to the film surface. The SAXS patterns show that the dried gel film is composed of crystal lamellae that are highly oriented with their large flat faces parallel to the film surface and within the lamellar crystals constituting the gel, the *c*-axes are oriented perpendicular to the large flat faces. Thus when the as-cast gel films are dried by slow evaporation of the solvent, the constituent lamellar crystals become oriented parallel to the film surfaces in a manner similar to mats of single crystals.

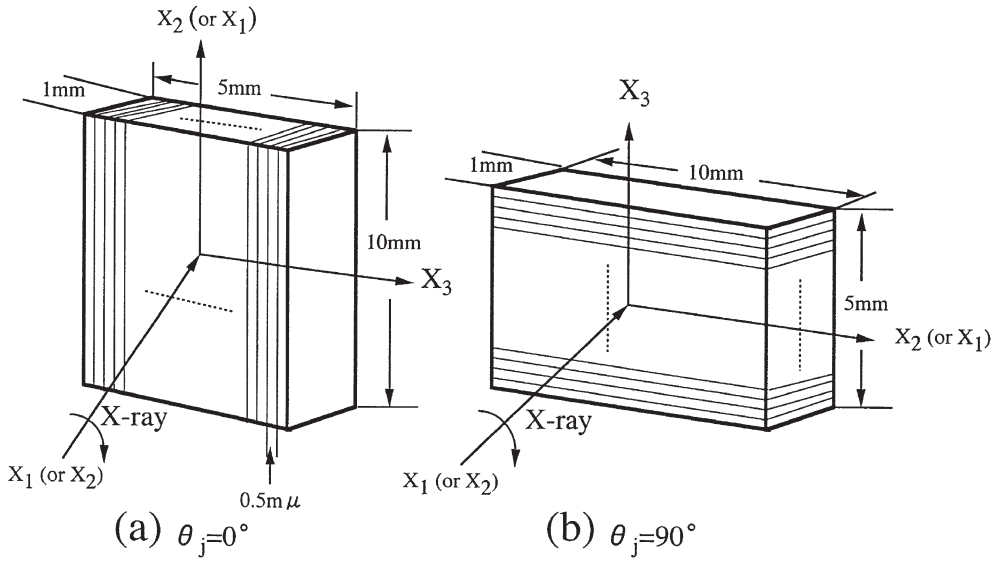

Figure 1. A number of thin stacked films to measure X-ray diffraction intensity distribution as a function of twice the Bragg angle at (a) $\theta_j = 0°$ (b) $\theta_j = 90°$.

Table I. Draw ratio dependence of crystallinity and melting point (listed in ref 11)

Draw ratio	Crystallinity (%)	Melting point (°C)
1 × 1	85.2	144
2 × 2	57.6	141
8.7 × 8.7	67.5	141

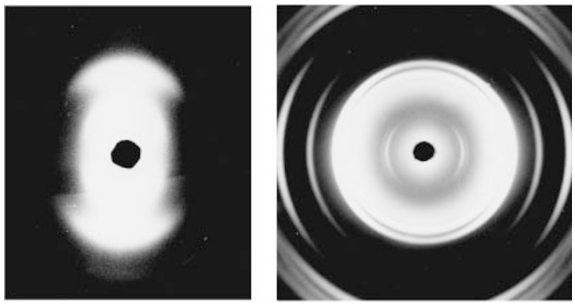

Figure 2. SAXS and WAXD patterns for the un-drawn dry gel film.

Figure 3 shows WAXS patterns (end view) of drawn films. The (110) and (200) planes with an orientation perpendicular to the film surface tend to orient parallel to the film surface. At 2 × 2, the (200) plane is oriented at 45° with respect to the film normal direction. At the maximum draw ratio 8.7 × 8.7, the (200) plane orients parallel to the film surface. In accordance with the orientational mode of the (200) plane, the (110) plane takes two modes. This mode was discussed elsewhere[11,16] and the mathematical geometrical arrangement shall be discussed later in this paper.

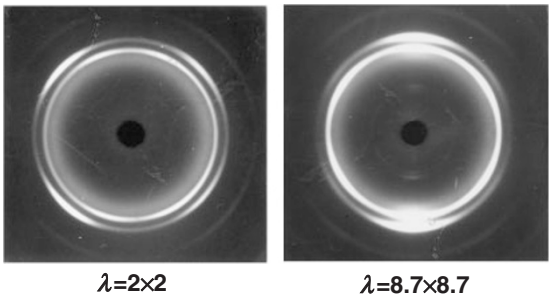

Figure 3. WAXD patterns (end view) of films with $\lambda = 2 \times 2$ and 8.7 × 8.7.

RESULTS AND DISCUSSION

General Concept

To simplify the present concept, efforts have been made to preserve the notation used in the previous paper.[10] The network chains will be assumed to be mono-disperse, *i.e.* composed of the same number m of rods having an ideal axial ratio x. The later dimensions of the rods will be of the size of solvent molecules or lattice sites. Figure 4a shows an illustrative network chain consisting of Kuhn segments (*i.e.*, freely jointed rods) between two successive cross-linked points. The U_3 axis parallel to the direction between the two cross-link points is specified with respect to the Cartesian coordinate 0-$X_1X_2X_3$ within the space of the film, the X_3 axis being the film thickness direction and the X_2 and X_3 plane being parallel to stretching directions, in which Θ is the polar angle between the U_3 and X_3 axes. In Figure 4b, the V axis denoting the direction of a given segment of a network chain is

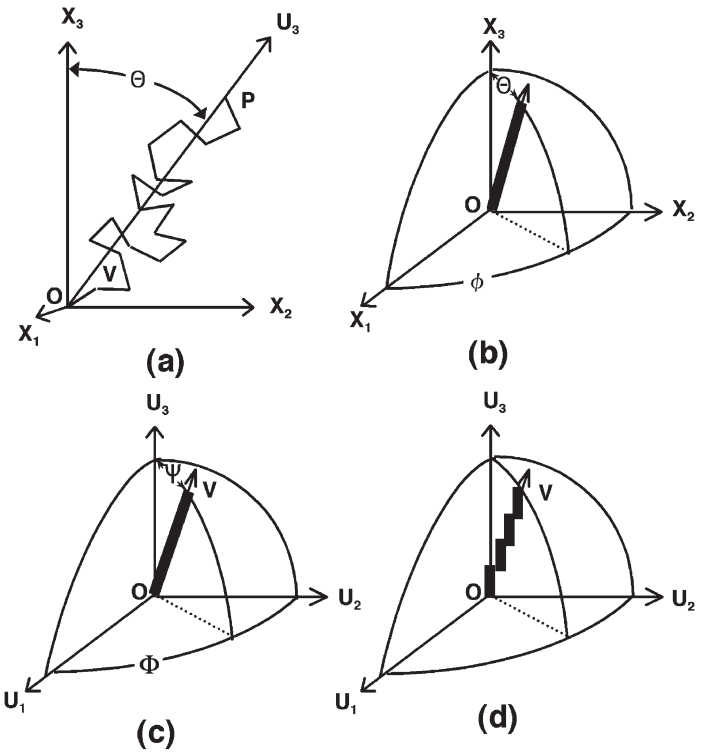

Figure 4. (a) Network chains of Kuhn segments between the two successive cross-linked points O and P. (b) Diagram illustrating the polar and azimuthal angles θ and ϕ, which specify the orientation of a segment of a chain with respect to Cartesian coordinate 0-$X_1X_2X_3$ fixed within the film space. (c) Polar angle Ψ and azimuthal angle Φ specify the orientation of a segment of a chain with respect to the Cartesian coordinate 0-$U_1U_2U_3$. (d) division of the segment into $y_k = x \sin \Psi$ sub-molecules, each oriented along the preferred direction.

defined by the polar angle θ and the azimuthal angle ϕ with respect to the Cartesian coordinate 0-$X_1X_2X_3$. The orientation of the segment is specified by the polar angle Ψ and the azimuthal angle Φ with respect to the Cartesian coordinate 0-$U_1U_2U_3$ as shown in Figure 4c, in which the U_1 and U_2 are chosen arbitrarily in the plane perpendicular to the U_3 axis. Following Flory *et al.*, the accommodation of the rod in the lattice is achieved through its representation by a sequence of $y_k = x \sin \Psi_k$ sub-molecules, each occupying x/y_k sites and oriented along the preferred direction, U_3 axis, as shown in Figure 4d. Thus, y_k characterizes the given rod. It is expressed in terms of Ψ_k and Φ_k as[8]

$$y_k = x \sin \Psi_k(|\cos \Phi_k| + |\sin \Phi_k|) \qquad (1)$$

for the rod exhibiting that particular orientation. Accordingly, the value of y_k increases as the rod becomes disoriented, as pointed out by Erman *et al.*[5] In their model system for uniaxially stretching, the preferred direction corresponds to the stretching direction between the two successive cross-linked points and the rods orient to the stretching direction without elongation in order to minimize the free energy of a given system, when the length-to-width ratio x of the Kuhn segment is beyond the critical value. Considering the Helmholtz free energy, this is undoubtedly reasonable for highly oriented chains to form a liquid crystal system and for highly oriented hard rods dispersed in a dilute solution. In spite of the rigorous treatment for the above systems in terms of the Helmholtz free energy, such a preferential orientation has never been observed for polymer films. To avoid this contradiction, the preferred axis was chosen along the direction between the two cross-linked points in the previous paper.[10] The treatment is similar to that of freely jointed chains of finite length represented by the distribution of Langevin.

For simultaneous biaxially stretching, such y_k also characterizes the spatial orientation of a given rod and is referred to as is disorientation index, the mean disorientation index, y, for the system of n_2 chains is defined by

$$y = \frac{1}{n_2 m} \sum_{l=1}^{n_2} n_{l,k} y_k \qquad (2)$$

where $n_{l,k}$ indicates the number of segments of the l-th chain, whose orientation lies within the k-th solid angle.

The total configurational partition function of a system of n_2 polymer and n_1 solvent molecules in a lattice consisting of n_0 sites ($n_0 = n_1 + mxn_2$) can be given by $Z_m = Z_{\text{comb}} Z_{\text{orient}}$, where Z_{comb} and Z_{orient}

are the combinational part of the partial function. The configuration partition function Z_m is used in the evaluation of the Helmholtz free energy change of mixing according to

$$\Delta A_m = -k_B T \ln Z_m \tag{3}$$

where k_B is the Bolzmann constant and T is the absolute temperature. According to Erman *et al.*,[5] $-\ln Z_{comb}$ is given by

$$-\ln Z_{comb} = n_1 \ln v_1 + n_2 \ln\left(\frac{v_2}{mx}\right) - (n_1 + n_2 my)\ln\left[1 - v_2\left(1 - \frac{y}{mx}\right)\right] + n_2(my - 1) - n_2(m - 1)\ln(z - 1) \tag{4}$$

where v_2 is a volume fraction of polymer given as mxn_2/n_0.

On the other hand, the orientational partition function Z_{orient} is given by

$$Z_{orient} = \prod_{j=1}^{n_2} m! \prod_k \frac{\omega_k^{n_{j,k}}}{n_{j,k}!} = \prod_{j=1}^{n_2}(n_{j,k}) \prod_k \frac{\omega_k^{n_{j,k}}}{n_{j,k}!} \tag{5}$$

where ω_k is the fractional range of the solid angle replaced by $(1/4\pi)\sin\Psi_k d\Psi_k$. Here, as discussed before,[10] it is evident that an equilibrium distribution of segments among different orientations is obtained by minimizing the free energy of the system with respect to $n_{j,k}$ to find the distribution of the probabilities of different configurations of segments in the network between the two cross-link points. The imposition of external constrains requires the use of Lagrange multipliers to minimize the free energy. Thus,

$$\frac{\partial}{\partial n_{j,k}}[\ln Z_m] = 0 \tag{6}$$

$$\sum n_{j,k} = m \tag{7}$$

$$\sum n_{j,k} \cos\Psi_k b = h \tag{8}$$

where b is the length of a segment and h is the distance between he two cross-link points. From eqs 7 and 8, we have

$$\alpha \sum \delta n_{j,k} = 0 \tag{9}$$

$$\beta \sum \cos\Psi_k \delta n_{j,k} = 0 \tag{10}$$

Substituting eqs 9 and 10 into eq 6, it takes the form

$$n_{j,k}/m\omega_k = \exp(\beta\cos\Psi_k - ay_k - 1) \tag{11}$$

Considering the difficulty in carrying out a double integration to determine β, the problem can be simplified to a considerable extent by pre-averaging Φ_k dependence prior to numerical integration over Ψ_k. Accordingly, y_k is given as $(4x/\pi)\sin\Psi_k$ and the distribution of eq 11 reduces to

$$n_{j,k}/m = (1/4\pi)\exp(\beta\cos\Psi_k - ay_k - 1)\sin\Psi_k d\Psi_k \tag{12}$$

where a is given by

$$a = -\ln\left[1 - v_2\left(1 - \frac{y}{x}\right)\right] \tag{13}$$

Accordingly, the distribution of eq 12 reduces to

$$n_{j,k}/m = (1/4\pi)\exp(\beta\cos\Psi_k - ay_k - 1)\sin\Psi_k d\Psi_k \tag{14}$$

The coefficients y/x and β in eqs 13 and 14 are needed to pursue numerical calculation. The complicated method to obtain them are described in Appendix I.

Application to Orientation Distribution Function of Amorphous Chain Segments under Simultaneous Biaxially Stretching

For freely jointed chains, the root-mean-square vector distance h_0 in the free state is related to

$$h_0 = mb^2 \tag{15}$$

When the sample is stretched to a draw ratio λ under a simultaneous biaxially elongation mode, the length h of the segment with the end-to-end vector of the length h_0 in the direction of Θ in Figure 4a becomes

$$h = \frac{h_0\lambda}{\{(\lambda^6 - 1)\cos\Theta^2 + 1\}^{\frac{1}{2}}} \tag{16}$$

Thus the orientation distribution function of the end-to-end vectors between the two cross-link points becomes

$$g(\Theta) = \frac{\lambda^3}{2\{(\lambda^6 - 1)\cos^2\Theta + 1\}^{\frac{3}{2}}} \tag{17}$$

For further development, it is convenient to have $f(\Psi)$ (see eq A-2) expanded in a series of spherical harmonics, *i.e.*,

$$f(\Psi) = \sum_{l=0}^{\infty} C_{l00}\Pi_l(\cos\Psi) \tag{18}$$

and

$$C_{l00} = \int_{-1}^{1} f(\Psi)\Pi_l(\cos\Psi)d(\cos\Psi) \tag{19}$$

where $\Pi_l(x)$ is the normalized polynominal. For numerical calculations, $f(\Psi)$ is expanded into the Taylor series up to the seventh order.

$$f(\Psi) = Q_0 \exp\{\beta \cos\Psi - (4xa/\pi)\sin\Psi\} = Q_0(Y)$$
$$= Q_0\{1 + Y + (1/2)Y^2 + (1/6)Y^3 + (1/24)Y^4 + (1/120)Y^5 + (1/720)Y^6\} \quad (20)$$

Here we shall define the orientation distribution function $\omega_{am}(\cos\theta)$ of segments with respect to the Cartesian coordinate 0-$X_1X_2X_3$ in Figure 4b. The function can be represented as a series of Legendre polynomials, *i.e.*,

$$\omega_{am}(\cos\theta) = \sum_{l=0}^{\infty} A_{l00}\Pi_l(\cos\theta) \quad (21)$$

with

$$A_{l00} = \int_{-1}^{1} \omega_{am}(\cos\theta)\Pi_l(\cos\theta)d(\cos\theta) \quad (22)$$

Considering the geometrical arrangement in Figure 4a–c, the angle θ between a segment and the stretching direction is related to Ψ, Φ, and Θ by

$$\cos\theta = \cos\Psi\cos\Theta + \sin\Psi\sin\Theta\cos\Phi \quad (23)$$

Application to the Legendre addition theorem to eq 23 led to

$$\Pi_l(\cos\theta) = \left\{\left(\frac{2}{2l+1}\right)^{\frac{1}{2}} \sum_{m=-l}^{l} \Pi_l^m(\cos\Theta)\Pi_l^m(\cos\Psi)\exp(-m\Phi)\right\} \quad (24)$$

From eq 22, it is seen that the coefficient A_{l00} is the average value of $\Pi_l(\cos\theta)$ for the segments. Therefore, A_{l00} is obtained if we multiply of sides of eq 24 by the orientation distribution functions, $\omega_{am}(\cos\theta)$, $g(\Theta)$, and $f(\Psi)$ and integrate over the whole range of θ, Θ, Ψ, and Φ. Hence,

$$A_{l00} = \left(\frac{2}{2l+1}\right)^{\frac{1}{2}} \sum_{m=-l}^{l} \int_0^{2\pi}\int_{-1}^{1} \Pi_l^m(\cos\Theta)\Pi_l^m(\cos\Psi)\exp(-m\Phi)g(\Theta)f(\Psi)d(\cos\Theta)d(\cos\Psi)d\Phi$$
$$= 2\pi\left(\frac{2}{2l+1}\right)^{\frac{1}{2}} \sum_{m=-l}^{l}\left[\frac{1}{2\pi}\int_0^{2\pi}\int_{-1}^{1} f(\Psi)\Pi_l^m(\cos\Psi)\exp(-m\Phi)d(\cos\Psi)d\Phi\right]\Pi_l^m(\cos\Theta)g(\Theta)d(\cos\Theta)$$
$$= 2\pi\left(\frac{2}{2l+1}\right)^{\frac{1}{2}} \int_{-1}^{1} C_{l00}g(\Theta)\Pi_l^m(\cos\Theta)g(\Theta)d(\cos\Theta) \quad (25)$$

Here l and m are even integers. The normalized associated Legendre's polynominal $\Pi_l^m(\cos X)$ and A_{l00} can be related to the associated Legendre's polynominal $P_l^m(\cos X)$ and the coefficient F_{l00} as follows:

$$P_l^m(\cos X) = \left(\frac{2}{2l+1}\right)^{\frac{1}{2}} \Pi_l^m(\cos X) \quad (26)$$

and

$$F_{l00} = \left(\frac{2}{2l+1}\right)^{\frac{1}{2}} 4\pi^2 A_{l00} \quad (27)$$

Substituting eqs 26 and 27 into eq 21, we have

$$4\pi^2\omega_{am}(\cos\theta) = \frac{1}{2} + 2\sum_{l=2}^{\infty}\frac{2l+1}{2}F_{l00}P_l(\cos\theta) \quad (28)$$

The actual calculation for the orientation distribution function of the amorphous chain segments was carried out by using eq 28.

The lattice model of a segmental orientation was also applied by Bahar *et al.*[6] to the thermotropic system with anisotropic polarizabilities. The treatment was first proposed by Flory[7,8] for thermotropic system with orientation-dependent interaction, and the theory is useful to explain the transition between crystallites, nematic, and isotropic phases for several polymers. The theory contains a factor of energetic character, which contributes to a first-order transition from a relatively disordered to a highly oriented structure, upon imposition of an external perturbation. In the present system, the new orientation function $f_t(\Psi)$ can be written as[10]

$$f_t(\Psi) = Q_0 \exp[\beta\cos\Psi - (4xa/\pi)\sin\Psi + ST^{-1}P_2(\cos\Psi)] \quad (29)$$

In eq 29, all the coefficients are described in Appendix II.

The orientation distribution function $\omega_{am}(\cos\theta)$ can be obtained by substituting $f_t(\Psi)$ into eq 25 instead of $f(\Psi)$ and by using eqs 26 and 27. This method is quite different from the concepts proposed by Bahar *et al.*[6] Following their concept, the preferred axis is fixed in a stable phase whose free energy is at a minimum with respect to the distribution of the orientation. Their numerical calculation for a thermal and un-deformed system in the case of chains consisting of $m = 20$ segments provided that the excess energy

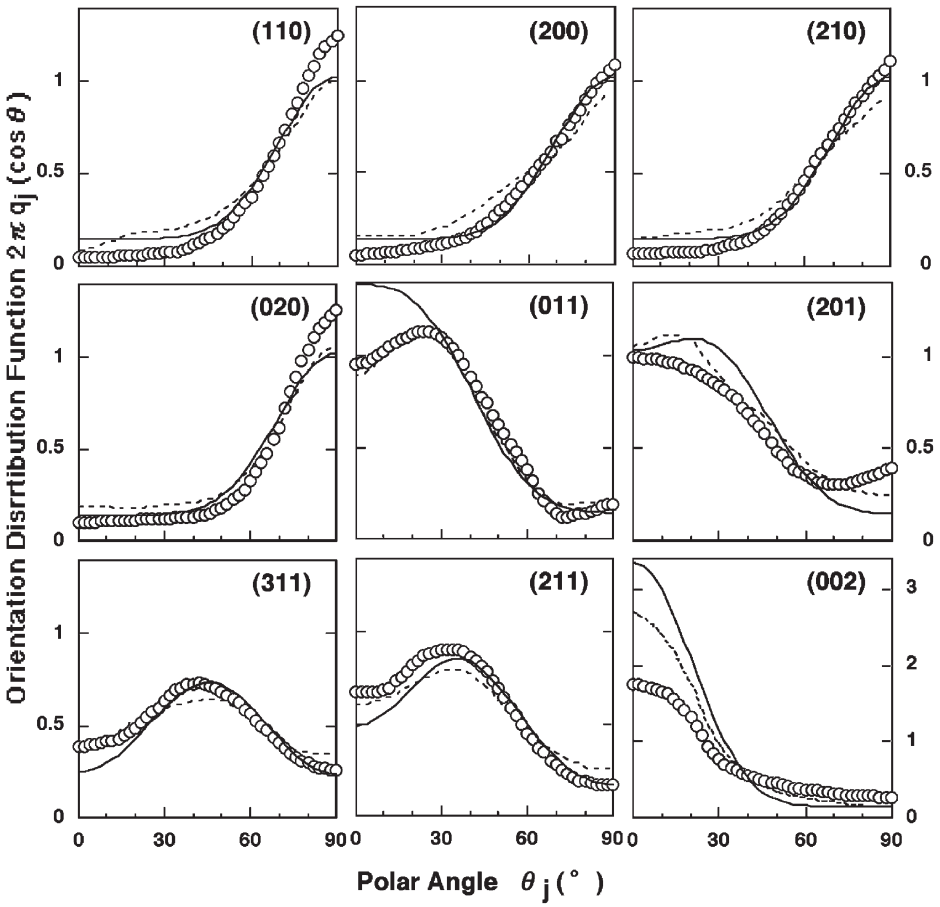

Figure 5. Orientation distribution functions $2\pi q_j(\cos\theta_j)$ of the reciprocal lattice vectors of the indicated crystal planes of an un-drawn polyethylene film. Circles: values of $2\pi q_j(\cos\theta_j)$ obtained from experimental measurements. Dashed curves: re-calculated by the method of Roe and Krigbaum, which were shown in ref 11. Solid curves: calculated theoretically from eq 35.

of the anisotropic phase gradually decreases and equates to that of the isotropic phase at $x = 6.42$, which means the axial ratio for the first-order phase transition from the isotropic to the anisotropic state. The calculation indicated that, for $x = 6.42$, the free energy of the anisotropic phase is less than that of the isotropic one and the anisotropic phase is the most stable phase and the second-order orientation factor was almost unity at $x > 10$, indicating almost perfect orientation. Surely, their treatments have advantage for the appearance of the appearance of anisotropic phase such as liquid crystal in the solution but have a problem to apply the deformation mechanism of polymer films and fibers.

In the present system, the amorphous chain segments take a random orientation, although the amorphous chain segments are oriented with respect to a preferred axis to minimize the Helmholtz free energy. This is due to the fact that for the present system, there are a number of the preferred axes within the film but the preferred axes are oriented randomly within an un-deformed film. Namely, at the large value of x, there exist partial orientation of amorphous segments as an assembly but the assemblies are oriented randomly within an un-deformed film. In this case, the second-order orientation factor is zero in an un-deformed state.

Application to Oriented Crystallization of Polyethylene under Simultaneous Biaxially Stretching

Figures 5–7 show the orientation distribution functions $2\pi q_j(\cos\theta_j)$ of the reciprocal lattice vector of nine crystal planes, which can be obtained directly by X-ray diffraction techniques, in which is a polar angle of the reciprocal lattice vector of the *j*th crystal plane with respect to the film normal direction (see Figure 8c). The adequacy of the present model can be judged by comparing the theoretical and experimental results. In doing so, the experimental accuracy of the measured values of $2\pi q_j(\cos\theta_j)$ must be estimated. The estimation was tried by using the re-calculated method proposed by Roe and Krigbaum.[17,18] The comparison between the experimental and re-calculated results was done in the previous paper.[11] As shown in the previous paper,[11] the re-calculated functions calculated from the orientation distribution function of crystallites were in good agreement with the observed functions, indicating that the experimental

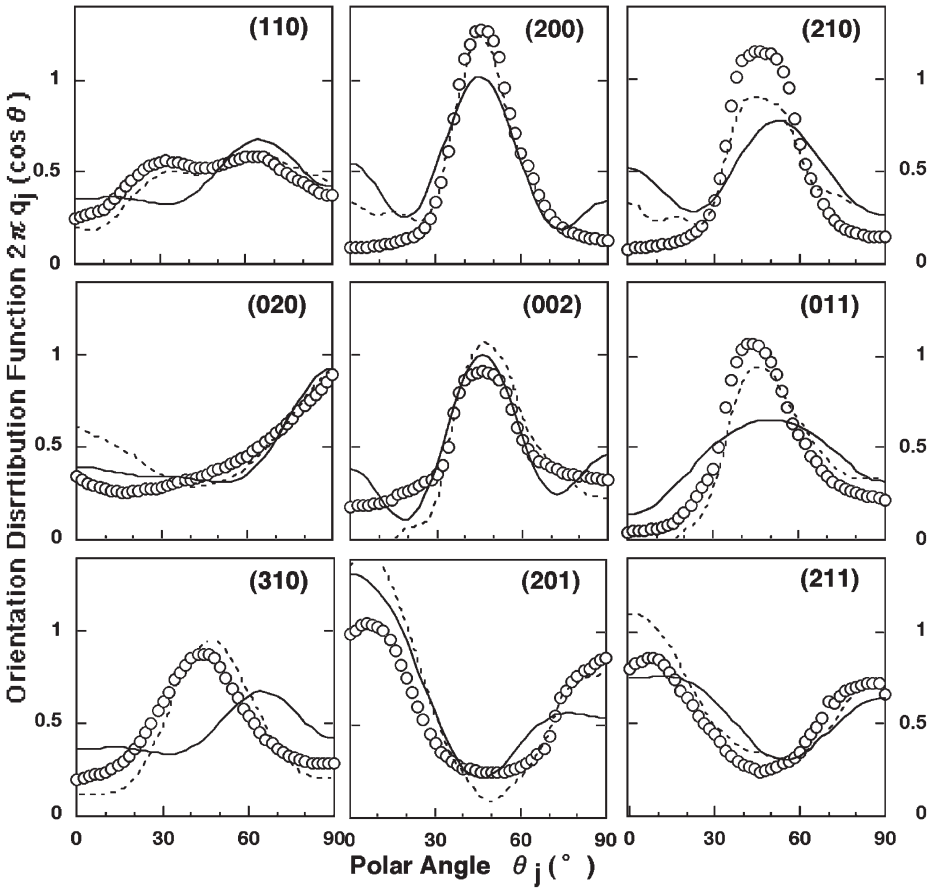

Figure 6. Orientation distribution functions $2\pi q_j(\cos\theta_j)$ of the reciprocal lattice vectors of the indicated crystal planes of an polyethylene film ($\lambda = 2 \times 2$). Circles: values of $2\pi q_j(\cos\theta_j)$ obtained from experimental measurements. Dashed curves: re-calculated by the method of Roe and Krigbaum, which were shown in ref 11. Solid curves: calculated theoretically from eq 39.

functions have high accuracy. To facilitate understanding the results, thes re-calculated curves are shown again as dotted curves in this paper. The values of a mean-square error obtained by the method of Roe and Krigbaum were 7.5% for $\lambda = 1 \times 1$, 8.3% at $\lambda = 2 \times 2$ and 8.9% at $\lambda = 8.7 \times 8.7$, respectively, as listed in the previous paper.[11] Accordingly, if the results calculated on the basis of segmental orientation by using a lattice model are in good agreement with the experimental curves, the present lattice model can be justified.

In previous paper,[10] oriented crystallization under uniaxial stretching was studied by using the lattice model in terms of the effect of amorphous chain segments by induced crystallization. The general concept proposed by Ziabick *et al.*[19–21] is due to the fact that the crystallization of amorphous chain segments depends on their orientation. This is based on the concept that a kinetically determined distribution of crystal chain axes as the normalized distribution of clusters found at the saddle point corresponding to a non-uniform orientation under conditions of a steady-state nucleation rate.

Following Hashimoto *et al.*,[21] the orientation of the *c*-axes, $W_c(\theta)$, was defined as a kinetically determined crystal orientation distribution function proportional to a normalized distribution of clusters with critical size r^* and l^*, which is given by

$$W_c(\theta) = \text{Const} \times \omega_{am}(\cos\theta) \exp\left\{-\frac{\Delta F(r^*, l^*, \theta)}{kT}\right\} \quad (30)$$

where $\Delta F(r^*, l^*, \theta)$ is the free energy at the saddle point, associated with the effective driving force of the cluster growth. In eq 30, the free energy needed to form a cylindrical cluster is given by

$$\Delta F(r, l, \theta) = 2\pi r^2 \sigma_c + 2\pi r l \sigma_s + \pi r^2 l\left[\Delta f - \left(\frac{kT}{v_0}\right) \ln \chi(\theta)\right] \quad (31)$$

where σ_c and σ_s are the end and the side surface free energies of polyethylene having values of 6.75×10^{-6} and 1.3×10^{-6} J/cm^2,[22] respectively, Δf is the bulk free energy of cluster formation, and v_0 is the volume of a single element, $\chi(\theta)$ is proportional to the possibility of finding a single element oriented at an angle θ within some finite tolerance range and is nearly equal to $\omega_{am}(\cos\theta)$ denoting the orientation function of sin-

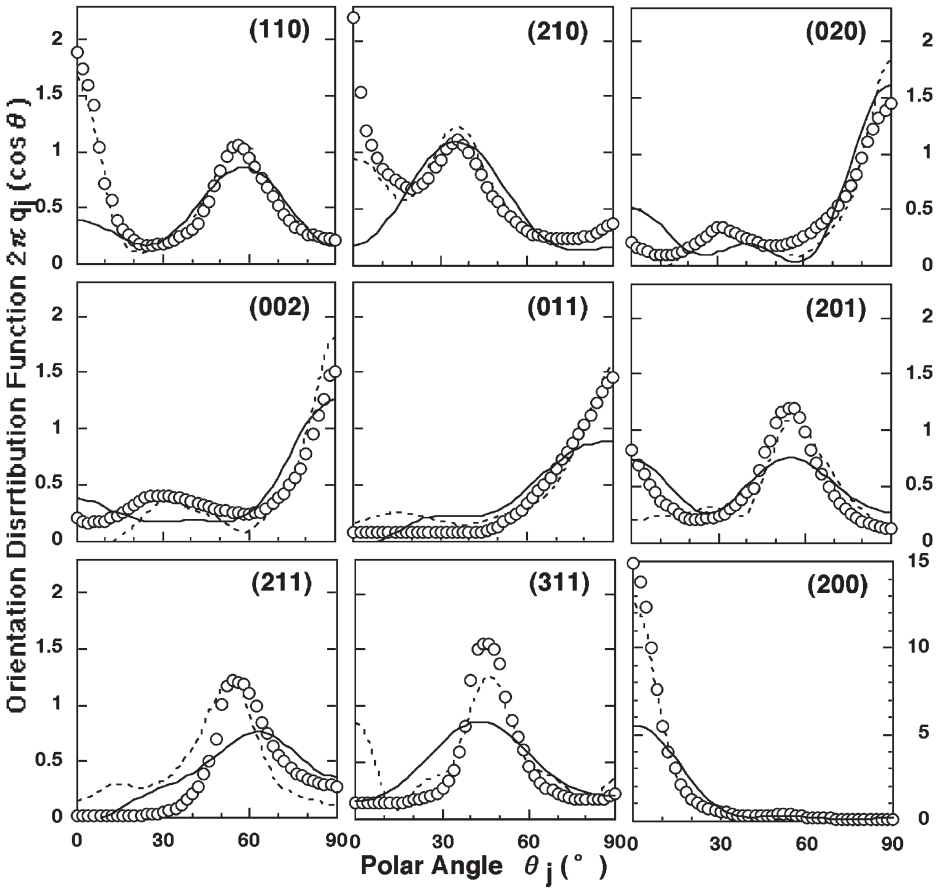

Figure 7. Orientation distribution functions $2\pi q_j(\cos\theta_j)$ of the reciprocal lattice vectors of the indicated crystal planes of an polyethylene film ($\lambda = 8.7 \times 8.7$). Circles: values of $2\pi q_j(\cos\theta_j)$ obtained from experimental measurements. Dashed curves: re-calculated by the method of Roe and Krigbaum, which were shown in ref 11. Solid curves: calculated theoretically from eq 40.

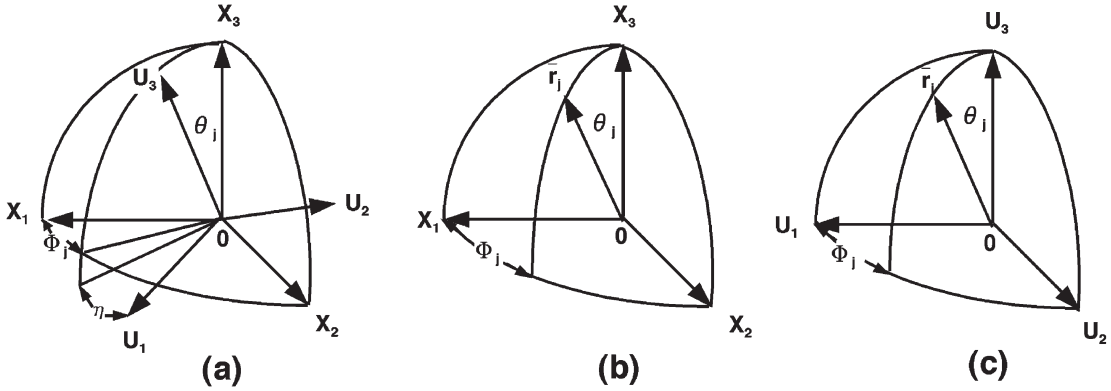

Figure 8. Cartesian coordinate illustrating the geometrical relation (a) Euler angles, ϕ, θ, and η, which specify the orientation of coordinate 0-$U_1U_2U_3$ of structural unit with respect to coordinate 0-$X_1X_2X_3$ of specimen. (b) Angles θ_j and ϕ_j which specify the orientation of the given j-th axis of the structural unit with respect to the coordinate 0-$X_1X_2X_3$. (c) Angles Θ_j and Φ_j which specify the orientation of the jth axis of the structural unit with respect to the coordinate 0-$X_1X_2X_3$.

gle chain elements.

Substituting $\Delta F(r^*, l^*, \theta)$ into eq 30, we have

$$W_c(\theta) = C\omega_{am}(\cos\theta)\exp\left[-\frac{8\pi\sigma_c\sigma_s^2}{D(\theta)^2 kT}\right] \qquad (32)$$

where C is the normalization constant. The orientation-dependent function $D(\theta)$ can be obtained by using $\omega_{am}(\cos\theta)$ in eq 21 as follows:

$$D(\theta) = \Delta f - \left(\frac{kT}{v_0}\right)\ln\chi(\theta)$$
$$= \Delta f - \left(\frac{kT}{v_0}\right)\ln[4\pi\omega_{am}(\cos\theta)] \qquad (33)$$

Assuming Kuhn–Grun statistics for the segmental

orientation under simultaneous biaxially stretching, we have

$$\Delta f = \Delta f|_{\lambda=1} - \left(\frac{kT}{2N_s v_0}\right)\left(2\lambda^2 + \frac{1}{\lambda^4} - 3\right) \quad (34)$$

where $\Delta f|_{\lambda=1}$ is given by $\Delta h(T-{}^0_m)/T^0_m$, where Δh is the density of the heat of fashion and T^0_m is the equilibrium melting point.

In numerical calculations, the following values of the parameters were used: the enthalpy of melting per mole of statistical segments, 4.03 kJ/mol and the equilibrium melting point, 137.5 °C. The volume v_0 ($= \pi r^2 l$) of a single kinetic element is an unknown parameter, but the calculated results in the range (2–4) $\times$ 10^{-22} cm^3 were insensitive to the value used. Accordingly, we adopted the value 3×10^{-22} cm^3, which is similar to the value for rubber, as discussed in the previous paper.[10]

To facilitate understanding geometrical arrangement of the crystallites with in the film, a new Cartsian coordinates are proposed. Figure 8a shows a Cartesian coordinate 0-$U_1U_2U_3$ fixed within a structural unit (crystallite) with respect to another Cartesian coordinate 0-$X_1X_2X_3$ fixed in a film. The U_3 axis may be taken along the *c*-axis. Because of the simultaneous biaxially stretched film, the *c*-axes have a random orientation around the X_3 axis (the film normal direction). The orientation of the structural unit within the space of the film may be specified by three Euler angles, ϕ, θ, and η. The angles θ and ϕ, which define the orientation of the U_3 axes of the unit within the space, are polar and azimuthal angles, respectively, and η specifies the rotation of the crystal unit around the *c*-axis. Under uniaxial orientation, the orientation function is independent of ϕ. Coordinates (b) and (c) show a given *j*th axis r_j within the unit, specified by the polar angle θ_j and the azimuthal angle ϕ_j with respect to the Cartesian coordinate 0-$X_1X_2X_3$ and specified by polar angle Θ_j and Φ_j with respect to the 0-$U_1U_2U_3$ of the unit.

Crystalline polymers are generally heterogeneous and are composed of polymer chains aggregated randomly to form amorphous regions along with more or less regular regions comprising several different orders of crystalline structural units. Therefore, deformations such as rotation of a crystal unit due to straining of tie-chains must be taken into consideration in addition to the simple orientation of the *c*-axes given in eq 32. If the orientation of the crystallites actually followed a random orientation around the *c*-axis as given by eq 32, then all of the orientational functions for the $(h, k, 0)$ planes would show the same profile. However, the observed X-ray patterns for the $(h, k, 0)$ planes have unique characteristics for drawn polyethylene films and the present specimens also exhibit this characteristic behavior as is discussed below. A possible source of the rotational distortion is provided by the strain energy of anisotropic crystallites in a stress field in a deformed network. Thus, the orientation distribution function of the crystallites in the deformed sample may be formulated empirically by allowing rotation of the crystallites around the *c*-axis.

Based on the X-ray diffraction pattern shown in Figure 2 and the curves in Figure 5, the orientation distribution function of crystallites in un-deformed state is given by

$$\omega(\theta, \eta) = C_0 W_c(\theta)\{1 + \sigma_1 \cos^{2(JA-1)}\theta + \sigma_2 \sin^{2(JB-1)}\eta\} \quad (35)$$

where $W_c(\theta)$ is a constant independent of θ at $\lambda = 1$. The second term on the right side represents the orientation of the crystallites, in which the *c*-axes are oriented parallel to the film normal direction but the crystallites are oriented randomly around the *c*-axis. The third term is the random rotation of the *c*-axis. The third term represents a random orientation component of the *c*-axis and the preferential orientation of the *a*-axis perpendicular to the plane formed by the *c*-axis and the film normal direction. With increasing the values of parameter *JA*, the possibility of finding crystallites becomes higher at $\theta = 0°$. The parameters σ_1 and σ_2 express the ease of the rotation, and *JB* represents the sharpness of the distribution.

As discussed in the previous paper,[10] the orientation factors F_{l0n} of the crystallites may be obtained as follows:

$$F_{l0n} = \int_0^{2\pi}\int_0^{\pi} \omega(\theta, \eta) P_l^n(\cos\theta)\cos n\eta \sin\theta \, d\theta \, d\eta \quad (36)$$

The orientation factor F^j_{l0} of the *j*th crystal plane can be obtained by using F_{l0n},

$$F^j_{l0} = F_{l00}P_l^n(\cos\Theta_j) + 2\sum_{n=2}^{l}\frac{(l-n)!}{(l+n)!}F_{l0n}P_l^n(\cos\Theta_j)\cos n\Phi_j \quad (37)$$

where Θ_j and Φ_j are the polar and azimuthal angles specifying the orientation of the reciprocal lattice vector with respect to the Cartesian coordinate of a crystal unit (see Figure 8c). Thus, the orientation distribution function $2\pi q_j(\cos\theta_j)$ of the reciprocal lattice vector of the *j*th crystal plane is observed by substituting eq 37 into the following equations:

$$2\pi q_j(\cos\theta_j) = \frac{1}{2} + 2\sum_{l=2}^{\infty}\frac{2l+1}{2}F^j_{l0}P_l(\cos\theta_j) \quad (38)$$

Figure 5 shows the observed orientation functions $2\pi q_j(\cos\theta_j)$ (open circles) with the calculated functions (solid curves). The numerical calculation was

continued until a best fit was achieved within the capacity of the simplex method. As the result, the following parameters yielded the best fit: $\sigma_1 = 24.386$, $\sigma_2 = 0.0823$, $JA = 5$ and $JB = 15$. The functions $2\pi q_j(\cos\theta_j)$ are essentially in good agreement with the experimental results (open circles).

Based on the experimental curves of $2\pi q_j(\cos\theta_j)$ at $\lambda = 2 \times 2$ shown in Figure 6, the function $\omega(\theta, \eta)$ is given by

$$\begin{aligned}\omega(\theta,\eta) &= C_0 W_c(\theta)\{1 + \sigma_1 \cos^{2(JA-1)}\theta + \sigma_2 \sin^{2(JB-1)}\eta \\ &\quad + \sigma_3(\lambda - 1)(\sin\theta\cos\theta)^{2(JC-1)}\cos^{2(JD-1)}\eta\}\end{aligned} \tag{39}$$

The parameter fitting by simplex method provided the best fit: $\sigma_1 = 0$, $\sigma_2 = 0$, $\sigma_3 = 830200$, $JC = 9$, $JD = 5$. The second and third terms on the right side represent the orientation of crystallites in un-deformed state (see eq 35) and the fourth term is associated with the deformation representing the preferential orientation of the c-axis at $\theta = 45^\circ$. In this process, the rotation of crystallites around the c-axis acquire the great possibility of the orientation of the a-axis to be in the plane formed by the c-axis and the film normal direction. The preferential orientation of the c-axis at $\theta = 45^\circ$ indicates the orientation of the c-axis by the shear stress occurred under the elongation up to 2×2. The parameter expresses the ease of the rotation and JC and JD represent the sharpness of the distribution. The functions $2\pi q_j(\cos\theta_j)$ are fairly in good agreement with the experimental results (open circles) but among them the functions from the (110), (210) and (310) are not good. This indicates that the orientation behavior of crystallites represented by eq 39 is too simple to justify the real orientation behavior of crystallites of UHMWPE dry gel films.

Based on the experimental curves of $2\pi q_j(\cos\theta_j)$ at $\lambda = 8.7 \times 8.7$ shown in Figure 7, the function $\omega(\theta, \eta)$ is given by

$$\begin{aligned}\omega(\theta,\eta) &= C_0 W_c(\theta)\{1 + \sigma_1 \cos^{2(JA-1)}\theta + \sigma_2 \sin^{2(JB-1)}\eta \\ &\quad + \sigma_3(\lambda - 1)\sin^{2(JC-1)}\theta\cos^{2(JD-1)}\eta \\ &\quad + \sigma_4(\lambda - 1)\cos^{2(JE-1)}\eta \\ &\quad + \sigma_5(\lambda - 1)(\sin\theta\cos\theta)^{2(JF-1)}\sin^{2(JG-1)}\eta\}\end{aligned} \tag{40}$$

The parameter fitting by simplex method provided the best fit: $\sigma_1 = 0$, $\sigma_2 = 0$, $\sigma_3 = 0.1185$, $\sigma_4 = 4.437$, $\sigma_5 = 8.3394$, $JC = 2$, $JD = 9$, $JE = 12$, $JF = 9$ and $JG = 2$. In eq 40, the second and third terms on the right side represent the orientation of crystallites in un-deformed state (see eq 35) and the other terms are associated with the deformation. The fourth term represents the preferential orientation of the c-axis with respect to the stretching direction, while the fifth and sixth terms, the random orientation. Judging from the maximum values of these terms at $\eta = 0^\circ$, the a-axis are oriented in the plane formed by the c-axis and the film normal direction. The seventh term means the preferential orientation of the c-axis at $\theta = 45^\circ$ and $\eta = 90^\circ$, indicating that the orientation of the c-axes by shear stress under elongation becomes most significant when the a-axis are oriented predominantly perpendicular to the plane formed by the c-axis and the film normal direction.

Equations 39 and 40 indicates the different orientational modes. Especially, the great opportunity to take the preferential orientation of the c-axis at $\theta = 45^\circ$ is quite different. The great possibilities occurred at $\eta = 0^\circ$ and 90° for the films with $\lambda = 2 \times 2$ and 8.7×8.7, respectively. As discussed above, the a-axes are oriented within the plane formed by the c-axis and the film normal direction at $\lambda = 2 \times 2$, while the a-axes are oriented perpendicular to the plane. This indicates that the orientational mode of crystallites changed under the elongation up to higher draw ratio.

Figures 9a, b and c show contour maps of the orientation distribution functions $\omega(\theta, \eta)$ of the crystallites at $\lambda = 1$, 2×2 and 8.7×8.7, respectively. At $\lambda = 1$, the magnitude is the highest at $\theta = 0^\circ$ but no η-dependence because of very smaller value of σ_2 than σ_1 in eq 35. The function $\omega(\theta, \eta)$ estimated experimentally (see Figure 14a in ref 11) is different from the function $\omega(\theta, \eta)$ represented by eq 35.

At $\lambda = 2 \times 2$ and 8.7×8.7, the maps are similar to those shown in the previous papers (see Figure 14 in ref 11). Namely, the density in map (b) is the highest at $\theta = 45^\circ$ and $\eta = 0^\circ$, indicating that the c-axes orients at $\theta = 45^\circ$ with respect to the film normal direction (or the stretching direction) by rotating around their b-axes, leading to the occurrence of shear stress. Map (c) shows a density maximum at $\theta = 90^\circ$ and $\eta = 0^\circ$, indicating that the c-axes orient predominantly parallel to the film surface by the rotation of crystallites around the b-axes with further elongation from $\lambda = 2 \times 2$ to 8.7×8.7.

Comparing Figure 9 with Figure 14 (see ref 11), the orientation distribution functions described by eqs 35, 39 and 40 are too simple to represent real orientations of crystallites. Even so, the essential tendencies for the highest density are the same. Accordingly, the orientation behavior of UHMWPE dry gel film by simultaneous biaxially stretching can be represented as each simple mode represented in eqs 39 and 40.

In spite of slightly different profiles of $2\pi q_j(\cos\theta_j)$ and $\omega(\theta, \eta)$ between experimental and theoretical curves, it may be expected that the essential behavior

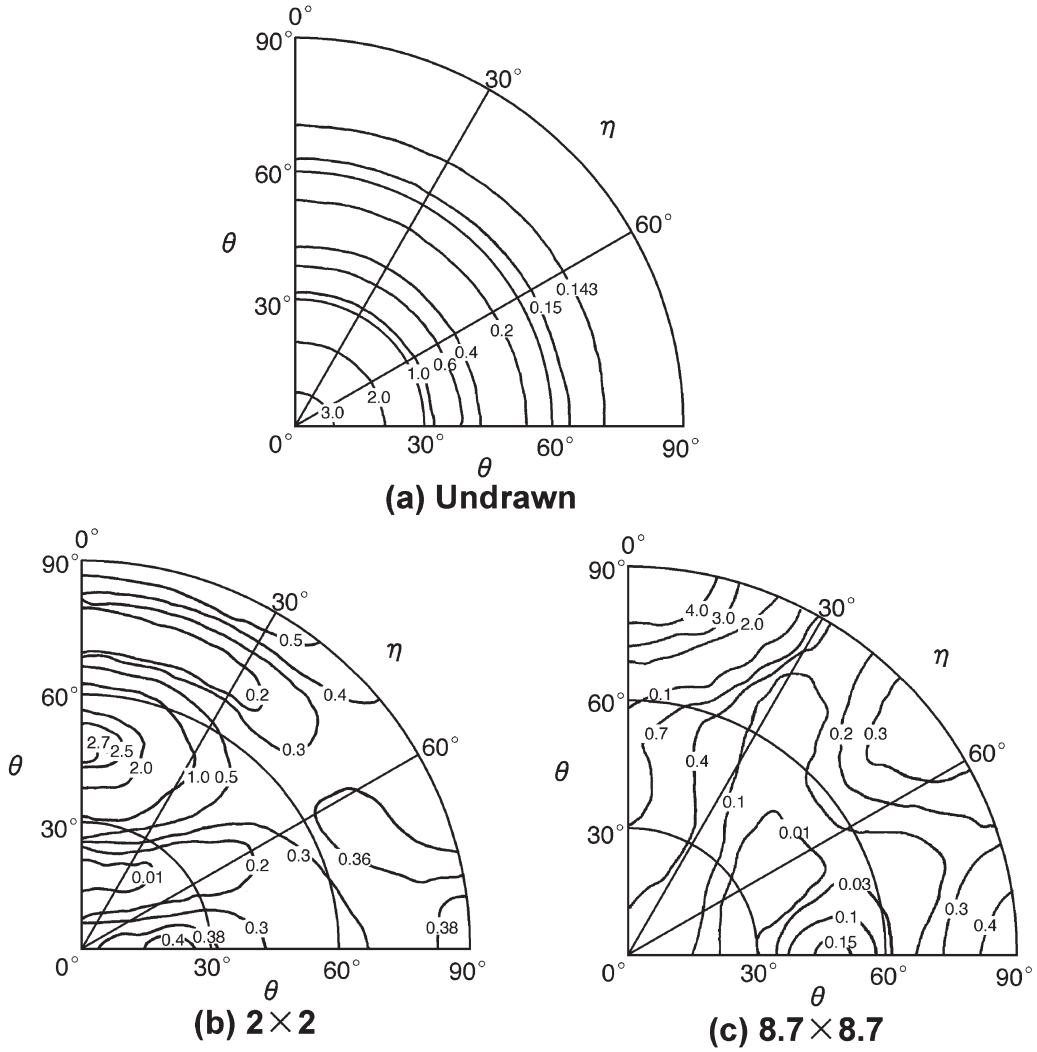

Figure 9. Orientation distribution functions of crystallites $4\pi^2\omega(\theta, \eta)$ calculated by eqs 35, 39 and 40 (a) un-drawn film (b) drawn film with $\lambda = 2 \times 2$ (c) drawn film with $\lambda = 8.7 \times 8.7$.

can be justified by the estimation of segmental orientation in deformed polymer networks using a lattice model as well as by a model concerning steady-state nucleation rate under the oriented crystallization of the segments under the elongation.

CONCLUSIONS

A lattice model was adopted to estimate the oriented crystallization of UHMWPE dry gel films under simultaneous biaxially stretching. The preferred axis associated with the preferred orientation of amorphous chain segments was chosen along the direction between two successive cross-linked points and the preferred axis was assumed to deform in an affine fashion with respect to the stretching direction. Accordingly, the orientation of amorphous chain segments was formulated in terms of the distribution function with respect to the stretching direction by using the Legendre additional theorem. Of course, the Helmholtz free energy of the anisotropic phase is less than the isotropic phase and the preferential orientation of the amorphous chain segments with respect to the direction between two successive cross-linked points achieves, when the length-to-width ratio of each chain segment increases beyond the critical point. As the application of the proposed model, the orientation distribution function of crystallites was calculated for UHMWPE dry gel film on the basis of the lattice model. The parameter fitting for the formulated orientation distribution function of crystallites was done for the film which was prepared by the gelation/crystallization from solution with 0.9 g/100 mL concentration, since the concentration assured the highest drawability under simultaneous biaxially stretching. The calculated orientation distribution functions $2\pi q_j(\cos\theta_j)$ of the reciprocal lattice vector of the crystal planes were in good agreement with the observed ones. Thus the numerical calculations indicated that the orientation of the *c*-axes depends on that of amorphous chain seg-

ments and the orientation behavior of crystallites is strongly affected by their rotation around the *c*-axis.

APPENDIX I

By using the condition imposed by the constrains, we have

$$\frac{h}{bm} = \frac{\int_0^{\pi} \exp[\beta \cos \Psi_k - (4xa/\pi) \sin \Psi_k] \cos \Psi_k \sin \Psi_k \, d\Psi_k}{\int_0^{\pi} \exp[\beta \cos \Psi_k - (4xa/\pi) \sin \Psi_k] \sin \Psi_k \, d\Psi_k} \tag{A-1}$$

Judging from eq 14, the orientation distribution function can be represented by omitting the dummy subscript k, which is as follows:

$$f(\Psi) = Q_0 \exp\lfloor \beta \cos \Psi - (4xa/\pi) \sin \Psi \rfloor \tag{A-2}$$

where Q_0 is a normalized constant given by

$$Q_0 = 1 \Big/ \int_0^{\pi} \exp[\beta \cos \Psi - (4xa/\pi) \sin \Psi] d\Psi \tag{A-3}$$

By expanding both the numerator and denominator in eq A-1 into Taylor series and keeping only the linear term of a and β reduces to

$$\frac{h}{mb} = \frac{\beta}{3(1 - ax)} \tag{A-4}$$

Based on $y = (4x/\pi) \sin \Psi$, we have

$$y = \frac{\int_0^{\pi} (4x/\pi) \exp[\beta \cos \Psi - (4xa/\pi) \sin \Psi] \cos \Psi \sin \Psi \, d\Psi}{\int_0^{\pi} \exp[\beta \cos \Psi - (4xa/\pi) \sin \Psi] \sin \Psi \, d\Psi} \tag{A-5}$$

By expanding the exponential part of both the numerator and the denominator in eq A-5 up to the second order in a and β, we have

$$\frac{y}{x} = \frac{1 - (32ax/\pi^2) + (\beta^2/8) + (2a^2x^2/\pi^2)}{1 - ax + (1/6)\beta^2 + (16a^2x^2/3\pi^2)} = 1 + ax\{1 - (32/3\pi^2)\} - \beta^2/24 \tag{A-6}$$

Using the approximation, we have

$$a = -\ln\left[1 - v_2\left(1 - \frac{y}{x}\right)\right] = v_2\left(1 - \frac{y}{x}\right) \tag{A-7}$$

From eqs A-6 and A-7, we have

$$a = \frac{1}{2x}\left\{\left(2 - \frac{d}{x}\right) - \sqrt{\left(\frac{d}{x}\right)^2 - \frac{4d}{x}}\right\} \tag{A-8}$$

where

$$d = 24\left\{1 - \frac{xv_2}{x_a}\right\}\frac{m^2b^2}{9v^2h^2} \tag{A-9}$$

and

$$x_a = \frac{1}{\left\{\frac{32}{3\pi^2}\right\} - 1} \tag{A-10}$$

APPENDIX II

In eq 29, S and T are given by

$$S = \frac{\int_0^{2\pi} f_t(\Psi) P_2(\cos \Psi) \sin \Psi \, d\Psi}{\int_0^{2\pi} f_t(\Psi) \sin \Psi \, d\Psi} \tag{B-1}$$

and

$$T^{-1} = \frac{k_B T}{x}\left[\frac{C z_c (\Delta\alpha)^2}{r.^6}\right]^{-1} \tag{B-2}$$

where z_c is the number of first neighbors surrounding the segments. $r.$ is the distance between subsegments for dense packing, and C is a constant.

By using a derivation similar to eqs A-6 and A-7, a is given by

$$a = \frac{1}{2x}\left\{2 - \frac{D}{U} - \sqrt{\left(\frac{D}{U}\right)^2 - 4\left(\frac{D}{U}\right)}\right\} \tag{B-3}$$

where

$$D = \left(\frac{dx}{8}\right) - d d_0\left(1 - \frac{T^{-1}}{5}\right) \tag{B-4}$$

$$U = \left\{d_0\left(1 - \frac{T^{-1}}{5}\right) + \frac{9dh^2}{15m^2b^2}\right\}x \tag{B-5}$$

$$d_0 = 8\left(1 - \frac{xv_2}{x_a}\right) \Big/ Tv_2 \tag{B-6}$$

Using the same treatment as shown in eqs A-5 and A-6, we have

$$\frac{y}{x} = 1 + ax\{1 - (32/3\pi^2)\} - \beta^2/24 - ST^{-1}/8 \tag{B-7}$$

From eq B-1, we have

$$S = \left\{\frac{ax}{8} + \frac{\beta x}{15}\right\} \Big/ \left\{1 - \frac{T^{-1}}{5}\right\} \tag{B-8}$$

REFERENCES

1. W. Kuhn and F. Grun, *Kolloid-Z.*, **101**, 258 (1942).
2. L. R. Treloer, *Trans. Faraday Soc.*, **36**, 881 (1954).
3. E. A. Di Marzio, *J. Chem. Phys.*, **36** 1563 (1962).

4. T. Tanaka and G. Allen, *Macromolecules*, **10**, 426 (1977).
5. B. Erman, I. Bahar, A. Kloczkowski, and J. E. Mark, *Macromolecules*, **23**, 5335 (1990).
6. I. Bahar, B. Erman, A. Kloczkowski, and J. E. Mark, *Macromolecules*, **23**, 5341 (1990).
7. P. J. Flory, *Proc. R. Soc. London, Ser. A*, **234**, 73 (1954).
8. P. J. Flory and G. Ronca, *Mol. Cryst. Liq. Cryst. Sci.*, **54**, 289 and 311 (1979).
9. D. Yoon and P. J. Flory, *J. Chem. Phys.*, **61**, 5366 (1979).
10. M. Matsuo, J. Ooki, Y. Harashina, T. Ogita, and R. St. J. Manley, *Macromolecules*, **28**, 4951 (1995).
11. T. Nakashima, C. Xu, Y. Bin, and M. Matsuo, *Polym. J.*, **33**, 54 (2001).
12. Y. Bin, K. Ooishi, K. Yoshida, T. Nakashima, and M. Matsuo, *Polym. J.*, **36**, 394 (2004).
13. P. Smith and P. J. Lemstra, *J. Mater. Sci.*, **15**, 505 (1980).
14. P. Smith, P. J. Lemstra, and H. C. Booij, *J. Polym. Sci., Polym. Phys. Ed.*, **19**, 877 (1981).
15. M. Matsuo and C. Sawatari, *Macromolecules*, **19**, 2036 (1986).
16. N. S. J. A. Gerrits and R. J. Young, *J. Polym. Sci., Part B: Polym. Phys.*, **29**, 825 (1991).
17. R. J. Roe and W. R. Krigbaum, *J. Chem. Phys.*, **40**, 2608 (1964).
18. W. R. Krigbaum and R. J. Roe, *J. Chem. Phys.*, **41**, 737 (1964).
19. A. Ziabicji and L. Jarecki, *Colloid Polym. Sci.*, **256**, 332 (1978).
20. M. Kosc and A. Ziabicki, *Macromolecules*, **15**, 1507 (1982).
21. T. Hashimoto, K. Saijo, M. Kosc, H. Kawai, A. Wasiak, and A. Ziabicki, *Macromolecules*, **18**, 472 (1985).
22. J. D. Hoffman, J. I. Lauritzen, E. Passaglia, Jr., G. S. Ross, L. J. Frolen, and J. J. Weeks, *Kolloid-Z.*, **231**, 564 (1969).